



# Shoreline change analysis and its application to prediction: A remote sensing and statistics based approach

Sabyasachi Maiti\*, Amit K. Bhattacharya

Department of Geology and Geophysics, Indian Institute of Technology, Kharagpur-721302, West Bengal, India

## ARTICLE INFO

### Article history:

Received 24 October 2007

Received in revised form 15 October 2008

Accepted 15 October 2008

### Keywords:

Shoreline change rate

Regression coefficient ( $R^2$ )

Root Mean Square Error (RMSE)

Shoreline prediction

Geomorphological evidences

## ABSTRACT

Shoreline change analysis and prediction are important for integrated coastal zone management, and are conventionally performed by field and aerial surveys. This paper discusses an alternative cost-effective methodology involving satellite remote sensing images and statistics. Multi-date satellite images have been used to demarcate shoreline positions, from which shoreline change rates have been estimated using linear regression. Shoreline interpretation error, uncertainty in shoreline change rate, and cross-validation of the calculated past shorelines have been performed using the statistical methods, namely, Regression coefficient ( $R^2$ ) and Root Mean Square Error (RMSE). This study has been carried out along 113.5 km of coast adjoining Bay of Bengal in eastern India, over the time interval 1973 to 2003. The study area has been subdivided into seven littoral cells, and transects at uniform interval have been chosen within each cell. The past and future shoreline positions have been estimated over two time periods of short and long terms in three modes, viz., transect-wise, littoral cell-wise and regionally.

The result shows that 39% of transects have uncertainties in shoreline change rate estimations, which are usually nearer to cell boundaries. On the other hand, 69% of transects exhibit lower RMSE values for the short-term period, indicating better agreement between the estimated and satellite based shoreline positions. It is also found that cells dominated by natural processes have lower RMSE, when considered for long term period, while cells affected by anthropogenic interventions show better agreement for the short-term period. However, on regional considerations, there is not much difference in the RMSE values for the two periods. Geomorphological evidence corroborates the results. The present study demonstrates that combined use of satellite imagery and statistical methods can be a reliable method for shoreline related studies.

© 2008 Elsevier B.V. All rights reserved.

## 1. Introduction

The shoreline, occurring between land and sea, is dynamic in nature. It undergoes frequent changes, short term and long term, caused by hydrodynamic changes (e.g., river cycles, sea level rise), geomorphological changes (e.g., barrier island formation, spit development) and other factors (e.g., sudden and rapid seismic and storm events) (Scott, 2005). The study of the rate of change in shoreline position is important for a wide range of coastal studies, such as development of setback planning, hazard zoning, erosion-accretion studies, regional sediment budgets and conceptual or predictive modeling of coastal morphodynamics (Sherman and Bauer, 1993; Al Bakri, 1996; Zuzek et al., 2003).

The conventional techniques for determining the rate of change of shoreline position include: field measurement of present mean high water level, shoreline tracing from aerial photographs and topo-

graphic sheets; comparison with the historical data using one of the several methods, (viz., end point rate (EPR) (Fenster et al., 1993), average of rates (AOR), linear regression (LR), and jackknife (JK) (Dolan et al., 1991)). Methods have inherent errors that depend upon several factors, namely, accuracy in shoreline measurement, temporal variability of the shoreline, number of data points (measured shoreline positions), non-uniform interval of time between the shoreline measurements, total time span of shoreline data acquisition, and the method used. Linear regression (LR) method of determining shoreline position change rate is found to be important among all such techniques, as it minimizes potential random error and short term variability (cyclical changes) through the use of a statistical approach (Douglas and Crowell, 2000).

Recent advancements in remote sensing and geographical information system (GIS) techniques have led to improvements in coastal geomorphological studies, such as: semi-automatic determination of shorelines (Ryu et al., 2002; Yamano et al., 2006); identification of relative changes among coastal units (Jantunen and Raitala, 1984; Siddiqui, and Maajid, 2004); extraction of topographic and bathymetric information (Lafon et al., 2002) and their integrated GIS

\* Corresponding author. Tel.: +91 3222 281536.

E-mail address: [s.maiti@yahoo.co.uk](mailto:s.maiti@yahoo.co.uk) (S. Maiti).

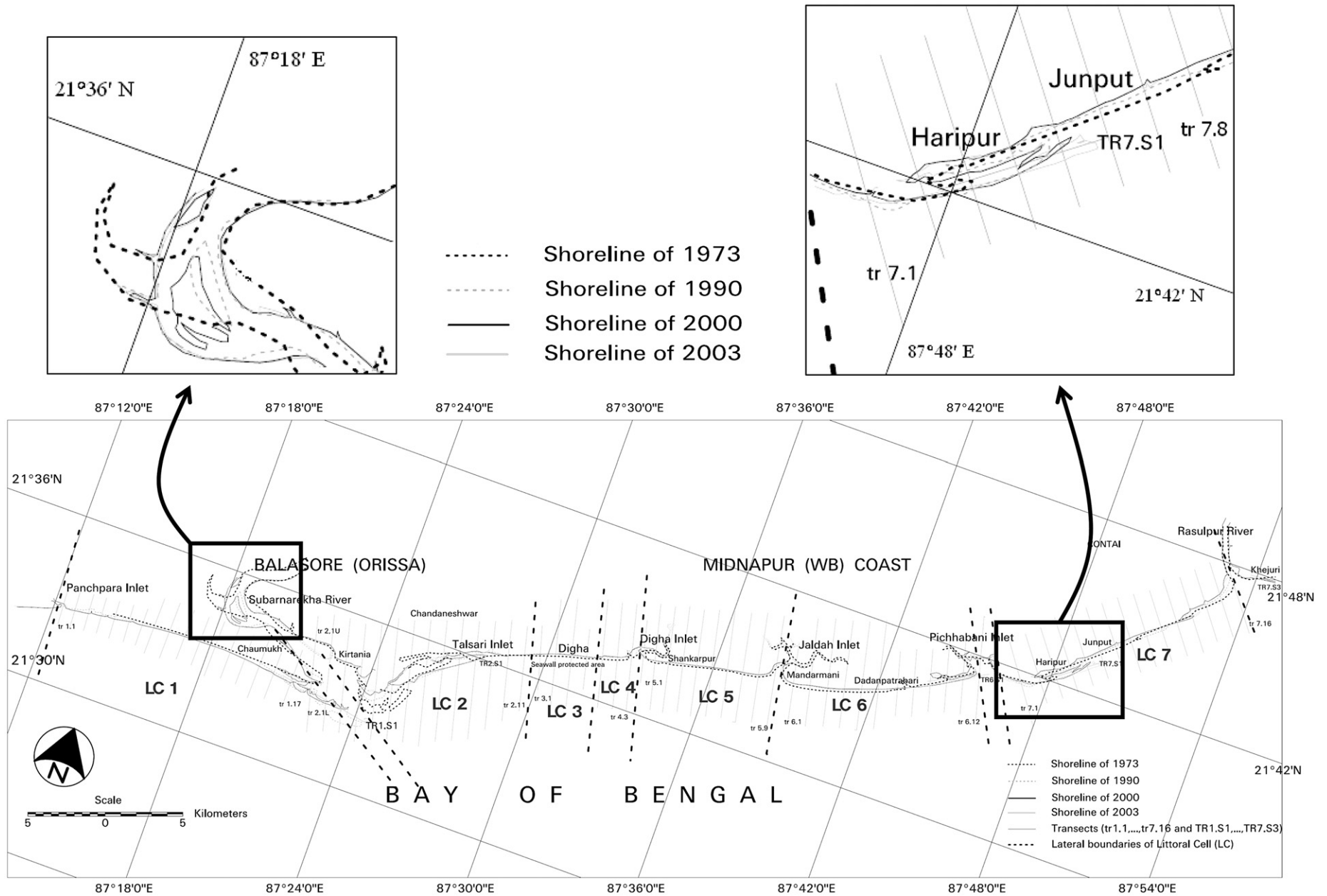


Fig. 1. Location map of the study area, shorelines positions (1973 to 2003), and transect lines (tr1.1 to tr7.16 and TR1.S1 to TR7.S2) and littoral cell (LC1 to LC7) boundaries. Close up boxes are shown for areas near LC1 and LC7.

analysis (White and El Asmar, 1999). These techniques are attractive, due to their cost-effectiveness, reduction in manual error and absence of the subjective approach of conventional field techniques.

In the present study, past shoreline change rates in the study area have been calculated, following the linear regression method. The estimated past shoreline positions were cross-validated using the Root Mean Square Error (RMSE) technique. Based on the estimated shoreline change rates, predictions of shoreline positions after short (13 year) and long (30 year) term intervals were carried out. The study area chosen in the present work is a 113.5 km long coastal stretch on the east coast of India, covering parts of Balasore and Midnapur littoral tracts occurring in Orissa and West Bengal States respectively, adjoining Bay of Bengal (Fig. 1). The western end of the study area is bounded by Panchpara Inlet in Balasore (Orissa), while Rasulpur River in Midnapur (West Bengal) forms the eastern boundary. One major river located in the study area is Subarnarekha River in Balasore. The predominant longshore current is oriented along the southwest-northeast direction. However, due to construction of groins and seawalls, this longshore sedimentation pattern is disturbed. Further, construction of dams on the Subarnarekha River has affected sediment supply. On the other hand, factors such as sea level rise, increase in storm frequencies as well as anthropogenic interferences had caused enhanced release of sediments from dunes and beaches, which in turn, had contributed towards the formation of offshore shoals and nearshore bars. Being located within the densely populated states of West Bengal and Orissa, this coastal stretch has become an important region of economic activities, viz., fisheries, tourism, construction of harbor and several small-scale industries, with passage of time. Clearly, an understanding of the spatial patterns of changes and availability of natural resources are prerequisites for an integrated management system of any coastal stretch.

The primary purpose of this work was to find the applicability of a combined technique of satellite image analysis and statistics in the prediction of future shoreline positions. In the present study, multi-resolution satellite images, which are easily available, have been utilized to demarcate shoreline positions during different times in the past. Statistical techniques, namely, Regression coefficient ( $R^2$ ) for finding change rate uncertainties, and Root Mean Square Error (RMSE) for cross-validation of back-calculated shoreline positions, were carried out in the present study. Based on estimated shoreline change rates, future predictions of shoreline positions have been calculated. Finally, an attempt has been made to corroborate the back-calculated error estimates with the geomorphologic observations.

## 2. Methodology

### 2.1. Data sources and geo-referencing

Multi-resolution satellite data over the study area, such as Landsat MSS, Landsat TM, Landsat ETM+ and ASTER of different dates have been acquired, as same resolution data is not available over the chosen period (1973 to 2003). The area is covered by five Survey of India (SOI, 1973) toposheets of 1973 at 1:50,000 scale, viz., Nos. 730/2, 730/6, 730/10, 730/13 and 730/14. The details regarding satellites and their acquisition dates and times are listed in Table 1.

The acquired satellite images have been georeferenced with the Survey of India toposheets of 1973, which have been regarded as the Reference Base Map. These are the highest resolution toposheets available for this study area. The potential shoreline positional error resulting from usage of small-scale toposheets for georeferencing has been taken into account in the selection of best grid resolution, as discussed below.

### 2.2. Selection of best grid resolution

Determination of a reliable shoreline reference feature (Coyne et al., 1999; Boak and Turner, 2005) using remote sensing techniques is very challenging due to various factors, viz., different ranges of tide induced variability (Ryu et al., 2002; Pajak and Leatherman, 2002), variations in meteorological conditions (Singh, 2002) and inequalities in pixel accuracies (Israel et al., 1997) during different periods of data acquisition (Table 1). These variations have been generalized in the present study by considering the data for calm sea conditions (Gourlay, 1996), uniform grid resolutions or pixel sizes for all considered satellite images (Hengl, 2006); and also by consideration of shoreline width up to the variable tide-affected width of the beach. The latter allows exclusion of tidal effects in shoreline mapping. Initially, in order to achieve best grid resolutions for all datasets, the area-wise (for each littoral cell, as considered in this study and described later) total amount of shoreline shift ( $A$ ) has been calculated using the relation (Allan et al., 2003):  $A = \text{difference in water level } (D) \times \text{beach slope of littoral cells}$ , where  $D$  is the difference of water level between the time of data acquisition and at high tide before the data acquisition. These data (tidal heights) for the entire study area have been collected from the nearest port, Sagar Island in the vicinity of the study area. Beach slopes at different places (covering littoral cells) have been collected from previous studies (Paul, 2002, 2006).

**Table 1**

List of different satellite data with acquisition date and time, tidal heights at acquisition times, sea level shifts, and littoral cell-wise variations in shoreline shifts

Sensor	Time (GMT +5:30)	Date of acquisition	Tide condition		SL <sup>a</sup> Shift from HT <sup>b</sup>		LC <sup>c</sup> wise total amount of shoreline shift (m)			
			Tidal height (ft)	Condition	(ft)	(m)	Digha (LC3 & 4) (1:47) <sup>d</sup>	Shankarpur (LC5) (1:55)	Dadanpatrbari (LC6) (1:43)	Junput (LC7) (1:72)
ASTER	4:55:58	December 3, 2003	7.46	Slack	5.44	1.66	77.93	91.24	71.31	119.38
ASTER	4:55:35	November 17, 2003	7.25	Rising	4.55	1.39	65.18	76.28	59.63	99.85
ASTER	4:49:16	November 10, 2003	15.4	Slack	0.21	0.06	2.86	3.35	2.62	4.39
ASTER	4:48:02	August 6, 2003	10.8	Rising	3.12	0.94	44.41	51.97	40.63	68.03
ASTER	4:49:16	June 3, 2003	15.8	Rising	0.51	0.15	7.16	8.38	6.55	10.97
ASTER	5:02:13	November 1, 2000	12.9	Rising	1.53	0.46	21.49	25.15	19.66	32.92
ASTER	5:03:10	September 30, 2000	17.88	Rising	0.12	0.04	1.72	2.01	1.58	2.63
ASTER	5:10:38	March 29, 2000	7.61	Rising	3.49	1.06	50.01	58.51	45.75	76.62
ETM+	5:30:08	November 8, 2000	8.11	Slack	5.79	1.76	82.95	97.06	75.89	127.06
TM	NA <sup>e</sup>	November 21, 1990	NA	NA	NA	NA	NA	NA	NA	NA
TM	3:38:00	November 14, 1990	12.45	Slack	1.75	0.53	25.07	29.33	22.94	38.41
MSS	3:38:00	January 17, 1973	13.45	Slack	0.45	0.14	6.45	7.54	5.92	9.88

<sup>a</sup> Sea level.

<sup>b</sup> High tide.

<sup>c</sup> Littoral cell.

<sup>d</sup> Beach slope for different cells (LC3... LC7) (Paul, 2002).

<sup>e</sup> Not available.

The above relationship of shoreline shift (Allan et al., 2003) in the present study, gives maximum shoreline shift ( $A$ ) of amount 127.06 m (Table 1) among littoral cells. Thus, a maximum width of 127 m of tide-inundated area has been considered. Based on this estimate, the Minimum Legible Delineation (MLD) (Hengl, 2006) of aerial extent  $127 \times 127 \text{ m}^2$  has been chosen in order to calculate the best grid resolution. The expressions,  $(\sqrt{a_{\text{MLD}}})$ ,  $(\sqrt{a_{\text{MLD}}/8})$ , and  $(\sqrt{a_{\text{MLD}}/4})$  (Hengl, 2006) have been applied to estimate the coarsest, finest and optimum resolutions of grid or pixel respectively, for the same MLD area ( $a_{\text{MLD}}$ ).

Based on these calculations, an optimum value of 63.5 m, between the coarsest value of 127 m and the finest value of 44.9 m has been selected in the present study. Hence, all satellite imageries have been resampled to a constant pixel resolution of 63.5 m by downsampling of Landsat TM (30 m), Landsat ETM (30 m) and ASTER (15 m), and upsampling of Landsat MSS (79 m) data.

### 2.3. Shoreline detection and digitization

Shoreline detections by automatic (Ryu et al., 2002; Loos and Niemann, 2002; Yamano et al., 2006) and manual digitization techniques are complicated due to presence of water saturated zones in the vicinity of the land water boundary. Initially in the present study, the shorelines have been identified and delineated using the processed NIR bands of Landsat MSS, Landsat TM, Landsat ETM+ and ASTER. The processing of the NIR bands included 'gray level thresholding' and 'segmentation by edge enhancement technique' (Lee and Jurkevich, 1990). The selected pixels, representing shorelines as described above, have been converted into vector layers. Uncertainties in some portions of the delineated shorelines were observed. To remove these uncertainties, in order to map continuous shoreline positions, other proxies, viz., 'dune toe' or 'vegetation line' (Fig. 2) (Zuzek et al., 2003) were carried out manually in stages. For example, if 'dune toe' failed to give satisfactory continuity of the shoreline

position at a particular portion of uncertainty, then 'vegetation line' proxy was used. Thus, finally the continuous shoreline positions during different periods (1973, 1990, 2000 and 2003) were drawn (Fig. 1).

### 2.4. Considerations of littoral cells and transects

Existing literature (Niyogi, 1970; GSI, 1995; Bhandari, 2001; Dey et al., 2002; Paul, 2002) indicates that the coast under study had evolved as sandy beach with gradual seaward progradation. The 113.5 km long coastal stretch under investigation has been broadly subdivided into seven 'littoral cells' (LC1 to LC7) with each 'cell' having uniform geomorphic, sedimentary (Sanderson and Eliot, 1999) and hydrodynamic characteristics. The inland boundaries of the littoral cells share the paleo-dune ridge or chenier complex of Subarnarekha River. The maximum height of this paleo-dune ridge has been attained along the present course of Subarnarekha River. This paleo-dune ridge gradually diminishes towards the western boundary of LC1 on the west, and around the middle of LC6 towards east. The paleo-dune ridge acts as chief source of beach sediment and releases its sediment due to frequent impact of storms. Other sediment sources are rivers and inlets; however, these natural openings are frequently obstructed by artificial interventions caused by irrigation and fishery projects. The cell boundaries (Cooper et al., 2001) are laterally bordered either by fixed boundaries, such as seawalls or groins (e.g., Old Digha) or by transient boundaries or natural openings, such as inlets, estuaries, or rivers, where tidal prisms or river discharges are expected to modify the longshore currents. The predominant longshore current moving from southwest towards northeast carries sediments and significantly modify the shoreline morphology. In offshore, the presence of numerous shoals act as both sink areas of littoral cells and seasonally as wind driven source of sediment. The hydrodynamic patterns are continuously changing with time due to gradual channel siltation and emergence of new islands in this part of Bay of Bengal. Thus, the complex

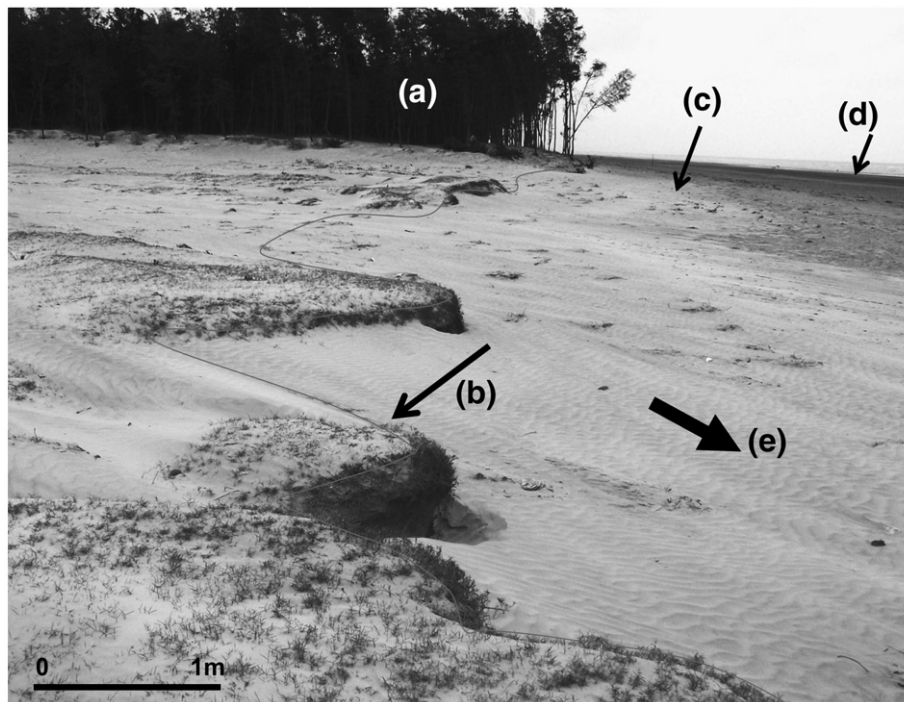


**Fig. 2.** Different types of shoreline reference features observed in LC7: (a) vegetation line (artificial plantation of vegetation over dune), (b) storm eroded shoreline position with discrete exposures of bluff line with consolidated sediment and grass, (c) high tide (HT) position of water, (d) position of water level during photography. The region between HT (c) and present water level (d) have relatively darker tone of water saturation, in comparison to dry sandy area (e). Temporary landward direction of aerodynamic ripple movement over dry sand is shown near (e).

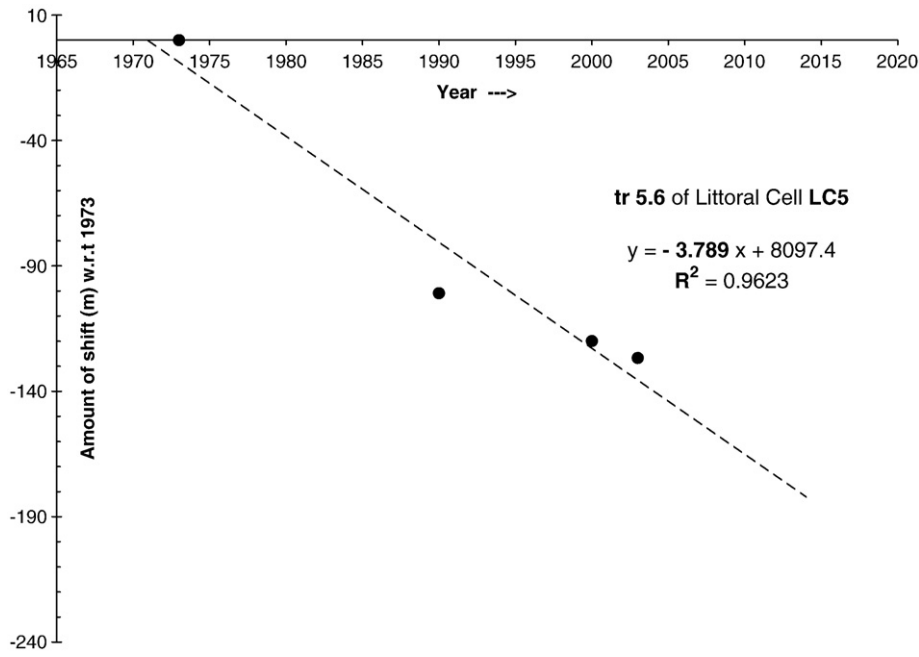


Fig. 3. Cross-plot of time versus amount of shoreline shift with respect to 1973 shoreline position, along transect (tr5.6) within littoral cell LC5.

morphodynamic pattern of this coast is not easy to ascertain by hydrodynamic modeling only. In addition, recent unplanned development of tourism, fisheries and irrigation projects have further disturbed natural coastal processes.

The seven littoral cells with their spatial extent are: (i) The first cell, LC1, of 28.8 km length, starts from the southwestern end of the study area, bounded by Panchpara Inlet and extends upto Subarnarekha River; (ii) LC2 of 15.2 km length, starts from the downdrift stretch of Subarnarekha River and extends upto Talsari Inlet, adjacent to the

seawall; (iii) LC3, 6 km long, covers Digha Development region comprising of seawall; (iv) LC4 of 3 km length, occurs between the seawall and Digha Inlet; (v) LC5, 8.7 km long, starts from Digha Inlet and extends upto Jaldah Inlet, (vi) LC6 of 20.6 km length, lies between Jaldah Inlet and Pichhabani Inlet; and finally (vii) the last cell, LC7, 31.2 km long extends from Pichhabani Inlet to Rasulpur River, at the northeastern end of the study area (Fig. 1).

Each littoral cell has been subdivided into a number of transects (e.g., tr1.1 to tr7.7), perpendicular to the shoreline of the reference

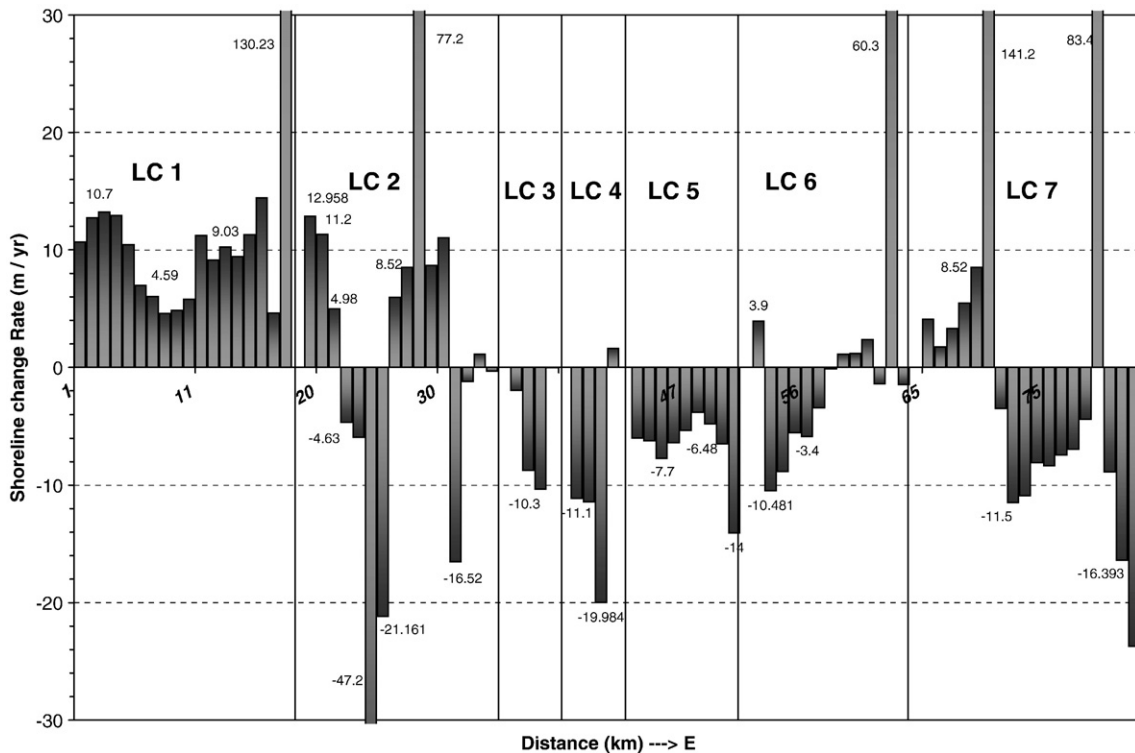


Fig. 4. Shoreline change rate distribution graph of littoral cells. Anomalous values of accretion rates (> 14 m/year), coinciding with transects nearer to spits or inlet migration, are followed by adjacent longshore (eastward) transects with erosion.

**Table 2**  
Detailed transect-wise description of calculated shoreline change rates (m/year), Regression coefficient values ( $R^2$ ) and 13 and 30 years' cross-validated RMS error, 13 and 30 years' hence future shoreline positions and geomorphological characteristics

Tr No.	Shoreline Change Rate (m/year)	$R^2$ <sup>a</sup>	Back calculated RMS error (m)		Future prediction (m)		Geomorphological characteristics
			13 years (1990)	30 years (1973)	13 years (2016)	30 years (2033)	
<i>Western boundary of Littoral cell 1 (LC1) and study area: Panchpara inlet</i>							
tr 1.1	10.66	0.96	322.94	na <sup>p</sup>	138.58	319.86	– Small inlets/drains/nala with lock-gates occupying most of the areas
tr 1.2	12.72	0.97	102.73	na	165.36	381.60	
tr 1.3	13.26	0.93	104.92	na	172.38	397.89	– Inlets are reclaimed with fisheries
tr 1.4	12.84	0.95	83.02	na	166.92	385.29	– Dunes mostly eroded in storm and local attempts of protections
tr 1.5	10.43	0.96	17.50	20.85	135.59	312.93	
tr 1.6	6.99	0.95	30.55	34.32	90.87	209.56	
tr 1.7	6.02	0.88	4.61	47.70	78.26	180.70	
tr 1.8	4.59	0.77	31.96	32.23	59.67	137.65	– Beach cusp
tr 1.9	4.86	0.77	23.54	14.48	63.18	145.82	
tr 1.10	5.80	0.84	3.09	72.84	75.4	174.38	– Accretion near western inlet boundary
tr 1.11	11.22	0.86	17.58	216.24	145.86	336.72	– Sand mining in places
tr 1.12	9.03	0.85	62.53	144.50	117.39	270.80	– Neo-dunes with sand-loving grasses
tr 1.13	10.24	0.88	44.67	196.30	133.12	307.08	
tr 1.14	9.32	0.86	150.81	72.63	121.16	279.51	
tr 1.15	11.28	0.90	130.01	55.51	146.64	338.37	
tr 1.16	14.37	0.89	36.64	242.35	186.81	431.22	– Spit advancement; landward erosion and opening of marshy areas
tr 1.17	4.63	0.79	177.08	na	60.19	138.85	– Spit advancement
TR1.S1	130.23	0.74	945.26	406.46	1693.00	3906.90	
<i>Boundary in between LC1 and LC2: Subarnarekha River</i>							
tr 2.1L	12.96	0.87	na	na	168.48	388.74	– Highly erosional by inlet processes
tr 2.1U	11.27	0.33	na	na	146.51	337.98	– Land reclamation (fisheries, salt-panning)
tr 2.2	4.98	0.91	88.55	202.64	64.74	149.55	– Sand mining in places
tr 2.3	–4.63 <sup>c</sup>	0.89	33.94	395.55	–60.19	–138.82	– Mangroves and its degradation in places
tr 2.4	–5.9	0.71	503.54	49.09	–76.70	–177.08	– Tidal creeks and channel
tr 2.5	–47.17	0.895	243.53	111.67	–613.21	–1415.00	– Salt marsh
tr 2.6	–21.16	0.84	179.69	380.25	–275.08	–634.83	– Groin construction
tr 2.7	5.94	0.67	64.52	409.00	77.22	178.35	
tr 2.8	8.5	0.14	282.90	700.11	110.50	255.44	– Eastward migration of inlet (Fig. 7a)
TR2.S1	77.2	0.93	na	226.45	1003.60	2315.91	
tr 2.9	8.68	0.91	183.05	86.72	112.84	260.29	– Deposition of barrier island
tr 2.10	10.92	0.85	118.61	300.82	141.96	327.57	– Erosion in downdrift of inlet migration
tr 2.11	–16.52	0.89	110.57	82.52	–214.76	–495.57	
tr 2.12	–1.197	0.06	81.86	180.42	–15.56	–35.90	
tr 2.13	1.12	0.45	5.99	9.52	14.56	33.71	
tr 2.14	–0.33	0.02	45.31	39.22	–4.29	–9.92	– Inlet upstream turned into fisheries
<i>Boundary in between LC2 and LC3: start of Sea wall</i>							
tr 3.1	–1.96	0.22	19.47	89.18	–25.48	–58.90	– Seawall (Fig. 5)
tr 3.2	–8.72	0.91	31.71	95.04	–113.36	–261.52	– Partially saturated beach near seawall
tr 3.3	–10.33	0.89	93.97	147.45	–134.29	–310.05	– Beach lowering
tr 3.4	–0.043	0.38	86.55	140.99	–0.56	–1.31	– Tourism (Fig. 9-I)
<i>Boundary in between LC3 and LC4: end of sea wall</i>							
tr 4.1	–11.1	0.96	61.46	185.58	–144.30	–332.97	– Highly erosional
tr 4.2	–11.42	0.91	72.14	129.90	–148.46	–342.63	– Sandbags dumping in places
tr 4.3	–19.98	0.96	94.89	161.13	–259.74	–599.52	– Land reclamation by fisheries
tr 4.4	1.62	0.47	44.20	308.44	21.06	48.59	– New groin to trap longshore sediments
<i>Boundary in between LC4 and LC5: Digha Inlet</i>							
tr 5.1	–5.99	0.42	64.20	17.71	–77.87	–179.82	– Erosion with older mudflat exposure (Fig. 8)
tr 5.2	–6.2	0.93	60.01	68.81	–80.60	–185.87	– Dredging near inlet mouth
tr 5.3	–7.71	0.92	53.83	73.99	–100.23	–231.17	– Dumping of Gabions for protections
tr 5.4	–6.37	0.91	48.78	70.24	–82.81	–191.00	
tr 5.5	–5.32	0.97	16.28	59.87	–69.16	–159.57	– Presence of remnant flood protection embankment in places
tr 5.6	–3.79	0.96	29.48	17.52	–49.27	–113.61	– Degradation of dunes
tr 5.7	–4.78	0.96	22.11	26.68	–62.14	–143.44	
tr 5.8	–6.48	0.96	42.02	9.62	–84.24	–194.48	
tr 5.9	–14.1	0.99	84.40	197.80	–183.30	–421.98	
<i>Boundary in between LC5 and LC6: Jaldah Inlet</i>							
tr 6.1	3.9	0.09	na	105.07	50.70	117.57	– Deposition (westward inlet migration)
tr 6.2	–10.5	0.94	159.33	34.81	–136.50	–314.43	– Erosion, with presence of beach cusp
tr 6.3	–8.82	0.94	92.78	85.99	–114.66	–264.60	
tr 6.4	–5.51	0.98	84.57	73.62	–71.63	–165.41	– Dune height gradually decreases
tr 6.5	–5.84	0.94	55.41	164.47	–75.92	–175.20	– Tourism
tr 6.6	–3.4	0.75	42.56	260.39	–44.20	–102.10	– Beach transportation activities (Fig. 9-II)
tr 6.7	–0.1	0.01	48.42	187.70	–1.30	–3.43	– Salt panning
tr 6.8	1.13	0.34	10.98	73.43	14.69	33.92	
tr 6.9	1.2	0.24	29.18	na	15.60	35.60	
tr 6.10	2.37	0.32	17.06	na	30.81	71.21	
tr 6.11	–1.4	0.05	53.09	na	–18.20	–41.93	– Deposition with sand-loving grass

Table 2 (continued)

Tr No.	Shoreline Change Rate (m/year)	R <sup>2</sup> <sup>a</sup>	Back calculated RMS error (m)		Future prediction (m)		Geomorphological characteristics
			13 years (1990)	30 years (1973)	13 years (2016)	30 years (2033)	
<i>Boundary in between LC5 and LC6: Jaldah Inlet</i>							
TR6.S1	60.3	0.98	na	68.81	783.90	1808.61	– Spit advancement; landward erosion
tr 6.12	–1.45	0.56	662.72	29.12	–18.85	–43.64	– Opening up of marshy inland channel
<i>Boundary in between LC6 and LC7: Pichhabani Inlet</i>							
tr 7.1	4.09	0.46	212.55	43.33	53.17	122.75	– Wind transported sand (Fig. 2) over eroded dunes from nearer offshore shoals
tr 7.2	1.75	0.22	17.64	131.30	22.75	52.50	
tr 7.3	3.3	0.44	153.30	242.81	42.90	98.95	
tr 7.4	5.47	0.96	59.34	294.89	71.11	163.97	– Small inlets/drains/nala with lock-gates
tr 7.5	8.52	0.53	29.86	na	110.76	255.58	
TR7.S1	83.39	0.94	461.16	321.61	1084.07	2501.76	– Eastward advancement of spit
tr 7.6	–3.48	0.52	49.02	93.01	–45.24	–104.31	– Marshy area (Fig. 7b); reclaimed by fisheries and salt-panning
tr 7.7	–11.49	0.89	52.24	115.42	–149.37	–344.73	
tr 7.8	–10.88	0.91	59.80	58.06	–141.44	–326.31	
tr 7.9	–8.07	0.94	49.03	56.28	–104.91	–241.96	– Mudflat advancement
tr 7.10	–8.34	0.78	152.98	165.47	–108.42	–250.37	– Reclaimed with fisheries
tr 7.11	–7.41	0.69	275.31	283.22	–96.33	–222.16	
tr 7.12	–6.92	0.54	40.56	266.23	–89.96	–207.47	– Flood protection embankment
tr 7.13	–4.36	0.16	33.33	147.76	–56.68	–130.97	
TR7.S2	141	0.99	157.42	na	1833.00	4230.00	– Eastward advancement of spit
tr 7.14	–8.86	0.65	208.01	93.66	–115.18	–265.92	– Opening up of marshy inland channel
tr 7.15	–16.4	1.00	174.41	179.88	–213.20	–491.79	
tr 7.16	–23.7	0.95	608.72	137.97	–308.10	–711.57	– Mudflat advancement
<i>Eastern boundary of LC7 [Eastern boundary of study area]: Rasulpur River</i>							

<sup>a</sup>Regression coefficient; <sup>b</sup>not available; <sup>c</sup>negative sign indicate erosion.

shoreline of 1973 at 1 km intervals. In addition, transects perpendicular to the tips of the spits (e.g., TR1.S1 to TR7.S2) have also been considered. A total of eighty two transects have been analyzed in the study area (Fig. 1 and Table 2).

### 2.5. Shoreline change rate calculation and prediction

The rate of change in shoreline position is an important parameter in the prediction of the future trend of shoreline shift. To measure the amount of shoreline shift along each transect, 1973 shoreline position (obtained from Landsat MSS) has been chosen as a baseline or zero (0) position. With reference to that baseline, seaward shifting of the shoreline

along transect is considered as a positive value, while landward shifting is considered as a negative value. All measurements along the same transect are plotted in a cross-plot, with 'year' plotted along the X-axis and the corresponding shoreline shift with respect to 1973 shoreline position plotted along Y-axis. In the cross-plots, positive trends indicate accretion, whereas negative trends as erosion. Fig. 3 represents a typical cross-plot with a negative trend for transect (tr5.6) of LC5. The plot also represents the linear regression equation as a measure of shoreline change rate and Regression coefficient (R<sup>2</sup>) as a measure of uncertainty. Thus, for the entire stretch of the coastline under study, the transect-wise information of shoreline change rate has been calculated and plotted (Fig. 4), in order to estimate both long and short terms shoreline changes.



Fig. 5. Seawall within LC3 with artificial mangrove plantation (white arrow) and boulders along beach (black arrow), as efficient barrier against coastal flooding and beach erosion.



the present study, an additional statistical method of measurement, namely, Root Mean Square Error (RMSE) has been undertaken for cross-validation of the estimated past shoreline positions.

### 2.6.3. Root Mean Square Error (RMSE)

Cross-validation of the estimated past shoreline positions is important in defining predictability and model quality. Calculation of Root Mean Square Error (RMSE) indicates how close the back-calculated dataset is to the actual. This error is calculated using the following relationship:

$$RMSE = \sqrt{\sum_{t=1}^n (\hat{y}_t - y_t)^2 / n} \quad (1)$$

where  $\hat{y}$  and  $y$  denote respectively, the calculated and the actual shoreline position at the  $t$ th transect for total  $n$  number of transects. Since cross-validation method is not affected by the number of data points, this method is more reliable than the Regression coefficient method. However, to avoid probable oversimplification in cross-validation estimates, selective geomorphological field checks should be carried out (Douglas et al., 1998). Any reduction in the sediment supply or changes in protection strategy or storms may significantly influence the cross-validation results; all these processes have incidentally taken place in the study area. Hence, in order to highlight these processes, RMSEs using Eq. (1), have been calculated at three levels, viz., individual transect-wise, littoral cell-wise, and regionally.

## 2.7. Identification of geomorphological characteristics

### 2.7.1. Using image processing techniques

Geomorphological characteristics could be ascertained through visual interpretation of satellite images, such as tonal changes in NIR and SWIR bands for water, wetlands, dry areas, planted vegetation and vegetated bodies of marsh; geometry of the shoreline; and associations of mudflats and sand units of beach, spit, bar, and shoal (SAC, 1992). Study of multi-temporal satellite images provides an overview of appearances and disappearances of different geomorphological features, changes in their spatial patterns, and probable inter-relationships. These observations are tabulated in Table 2.

### 2.7.2. Field observations

Field observations of geomorphological characteristics, shoreline reference features (Fig. 2) and man-made protection strategies (viz.,

seawall and its extension, planting of mangrove vegetation as shown in Fig. 5, and placement of sand bags at regions with low dune heights) were recorded and presented in Table 2.

The various steps followed in the present study are presented in the flowchart (Fig. 6).

## 3. Results and discussions

The results of the present study and the identified geomorphological characteristics are finally compiled and tabulated in Tables 2 and 3. In Table 2, transect-wise (eighty two) calculated shoreline change rates, Regression coefficient values, cross-validated Root Mean Square Errors, and predicted future shoreline positions along with geomorphological characteristics are presented. In Table 3, littoral cell-wise (seven) and regional (total) summary of the results are presented, highlighting the following items: lengths of cells, number of transects within each cell, shoreline change rate statistics (mean, maximum, minimum and standard deviation), percentage of transects that record erosion, accretion and statistical uncertainty, cross-validated RMSE, and predicted average shoreline shift.

### 3.1. Predicted shoreline positions

A brief discussion of the results, presented in Tables 2 and 3 and shown in Fig. 7, is given below.

The first cell, LC1, on the extreme southwestern end of the study area shows overall accretion (all transects); additionally, downdrift advancement of a spit near the eastern boundary of this cell is observed. The next cell, LC2, exhibits both erosion (43.8% of transects) and accretion (56.2% of transects), and downdrift migration of an inlet near the eastern end. Crossing this inlet, the area turns gradually into an 'erosional hotspot' for the next 18 km coastal stretch comprising littoral cells, LC3, LC4 and LC5. Among these three cells, the highest amount of erosion is predicted for cell LC4, surrounding Digha Inlet. 'Erosional hotspot' regions are found to have artificial protections, created by construction of seawalls and groins, and dumping of sandbags and gabions. These protections have caused localized beach accretion, beach lowering and severe erosion at several places. For example, as seen in Fig. 8, in case of LC5, beach lowering has occurred due to abrasive movement of a thin layer of sand over older mudflat. Inlets within this hotspot region are disturbed by anthropogenic activities (lock-gates' controls of tides, fisheries, dredging etc.) causing inlet movement opposite to drift direction. The next cell, LC6, shows

**Table 3**  
Regional and littoral cell-wise statistical summary of shoreline change rate information

	LC1	LC2	LC3	LC4	LC5	LC6	LC7	Regional (total)
Total number of transects	18	16	4	4	9	13	18	82
Shoreline length (km)	28.8	15.2	6	3	8.7	20.6	31.2	113.5
Mean rate shoreline change rate (m/year)	16.03	2.79	-5.26 <sup>a†</sup>	-10	-6.74	2.45	7.7	4.75
Minimum rate shoreline change rate (m/year)	4.59	-47.2	-10.3	-20	-14.1	-10.5	-23.7	-47.17
Maximum rate shoreline change rate (m/year)	130.2	77.2	-0.04	1.62	-3.79	60.3	141	141
Standard deviation of rates (m/year)	28.68	25.1	5.03	8.9	2.96	17.9	40.1	27.38
Total transects that record erosion	0	7	4	3	9	8	11	42
Total transects that record accretion	18	9	0	1	0	5	7	40
Total transects that record statistical uncertainty ( $R^2 < 0.8$ )	4	7	2	1	1	8	9	32
Total transects considered for RMS error comparison ( $n=68$ )	13	13	4	4	9	9	16	68
Total transects showing lesser RMS error (seen for 13 years period)	9	8	4	4	6	5	11	47
% of total transects that record erosion	0	43.8	100	75	100	61.5	61.1	51.2
% of total transects that record accretion	100	56.3	0	25	0	38.5	38.9	48.8
% of total transects that record statistical uncertainty ( $R^2 < 0.8$ )	22.2	43.8	50	25	11.1	61.5	50.0	39.02
% of total transects showing lesser RMS error (seen for 13 years period)	69.2	61.5	100	100	66.7	55.6	68.8	69.12
Cross-validation of 1990 (13 years past) RMS error (m) ( $N=77$ )	248.1	197.5	66.5	70.6	51.1	202.4	219.6	198.6
Cross-validation of 1973 (30 years past) RMS error (m) ( $N=70$ )	163.8	293.3	121	207.6	81.2	128.9	186.7	191.5
Predicted average shoreline shift amount (m) after 13 years	208.4	36.3	-68.4	-132.9	-87.7	31.9	99.4	12.4
Predicted average shoreline shift amount (m) after 30 years	480.8	83.8	-157.9	-306.6	-202.3	73.6	229.3	28.7

<sup>a†</sup> Negative sign indicates erosion; 'n' is number of transects considered for comparison between 13 and 30 years; 'N' is total number of transects considered for individual periods.

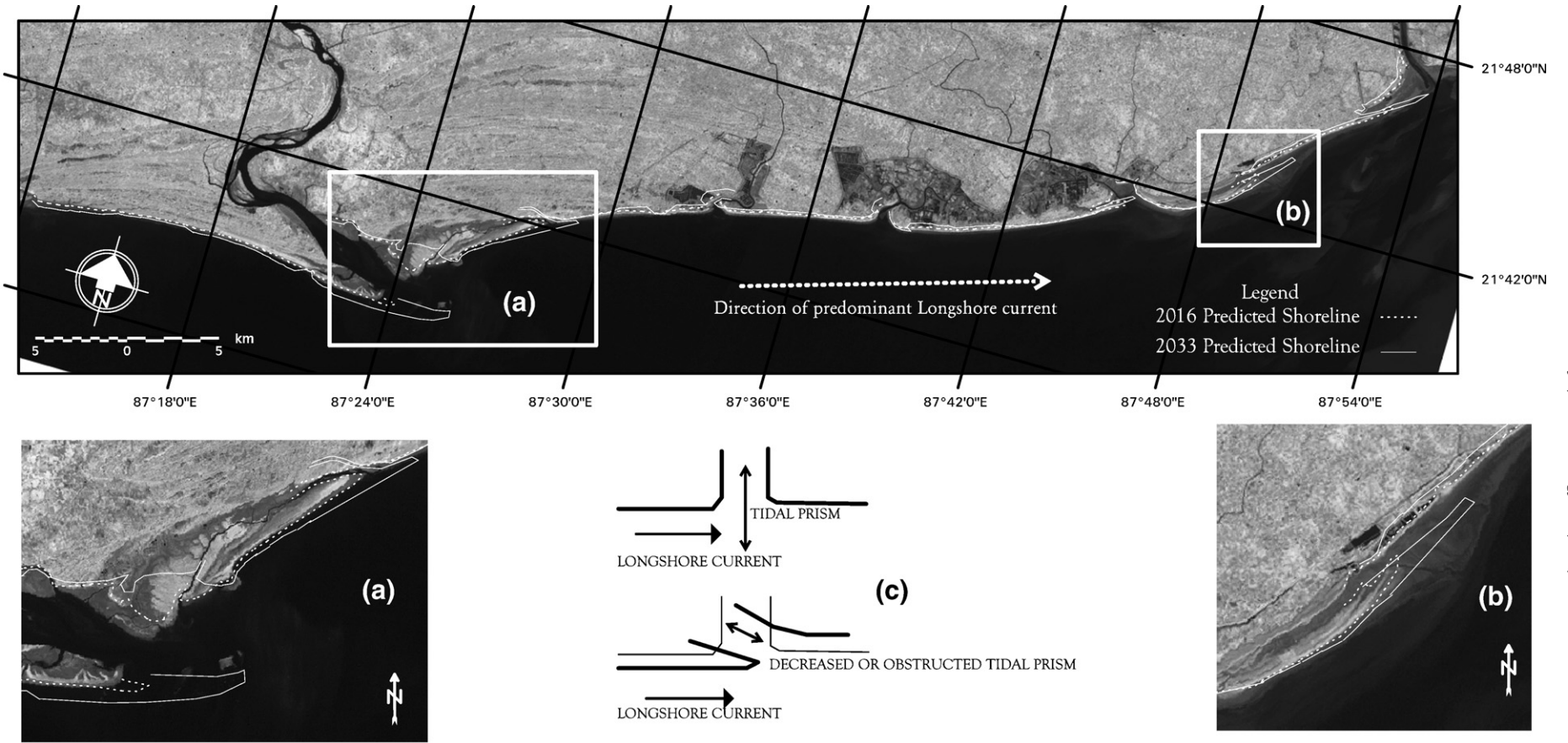
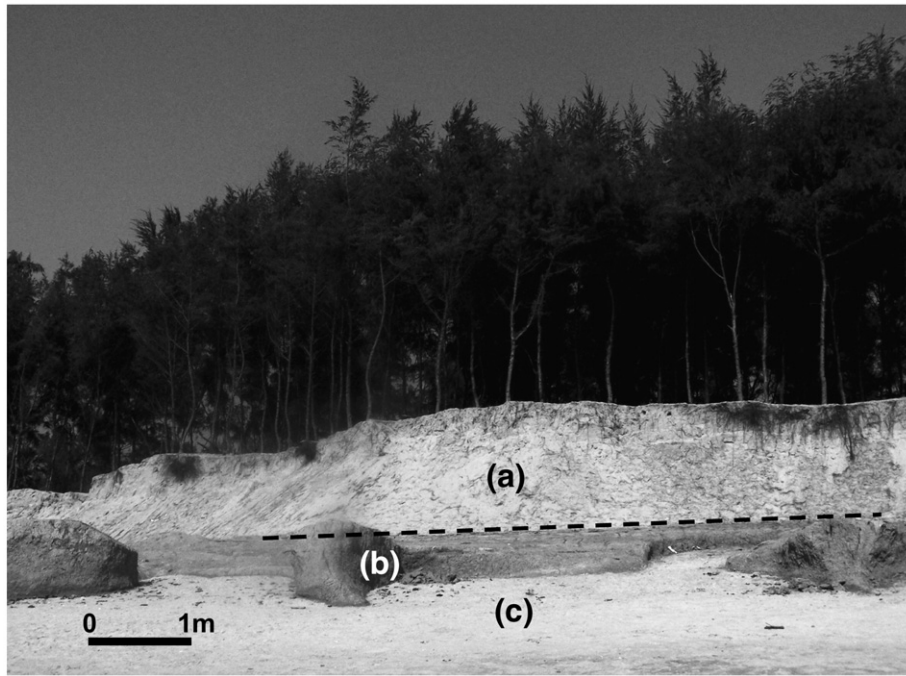


Fig. 7. Prediction of 13 and 30 years henceforth shoreline position. Magnifications near (a) inlet migration, and (b) spit development; (c) expected morphodynamic model.



**Fig. 8.** Dunes at LC5 severely eroded with remnant tree roots and exposed mud layer (b), underlying dune (a). Black dashed line marks the boundary between (a) and (b). Sand particles near foreshore region (c) act as abrasive agents. The photograph is digitally enhanced to differentiate mud and sand layers.

mixed erosion (61.5% of transects) and accretion (38.5% of transects). This cell also has spit development near eastern boundary. The last cell, LC7, also shows both erosion (61.1% of transects) and accretion (38.9% of transects) with development of two spits in the middle of the cell.

The predicted future shoreline positions have been also based upon a conceptual morphodynamic model (Bruun et al., 1978; FitzGerald et al., 2000; Short, 2001; McBride et al., 2007), in addition to the estimated past shoreline change rate. According to this model, an inlet opening was initially orthogonal to the shoreline as long as tidal prism was high. However, with the decrease of tidal prism (SPM, 1984; CEM-II-6, 2002), caused by artificial obstructions, this inlet opening was disturbed from its original orthogonal orientation, and changed to oblique orientation with the shoreline (Fig. 7c). This model is particularly valid for the development of spits and associated erosion (Fig. 7a and b).

### 3.2. Validation of results by statistical techniques

Cross-validations of change rate estimations and back-calculated shoreline evaluations have been carried out using statistical techniques, namely, Regression coefficient ( $R^2$ ) and Root Mean Square Error (RMSE). In Table 2, low Regression coefficient values ( $R^2 < 0.8$ ) are observed; these low values indicate uncertainty of shoreline change rate measurement with 39.02% of transects having low values (Table 3). These uncertainties are mainly for transects adjacent to estuaries, inlets, tidal creeks, spits, or shoals.

On the other hand, RMSE values (Table 2) occur over a very wide range, from 3.09 m to 945.26 m. A comparative analysis of the RMSE values, calculated for the two periods (13 and 30 years), have been done in three modes, viz., transect-wise, littoral cell-wise and regionally to arrive at meaningful inferences vis-à-vis geomorphological observations. As observed in Table 2, RMSE values could be calculated for 77 of the transects only ( $N=77$ , Table 3) in the case of the 13 year interval, and for 70 transects only ( $N=70$ , Table 3) for the 30 year interval, due to non-availability of the shoreline positions for some of the transects (e.g. for tr1.1, tr1.2, tr2.1 etc, marked 'na').

When transect-wise comparison of RMSE values for the two periods was attempted, it was observed that only sixty eight number of transects have RMSE values for both periods (Table 2;  $n=68$ , Table 3), and 47 of the transects (i.e., 69.12% of considered transects) show lower RMSE values for the 13 year interval than that for the 30 year interval (Table 3). Likewise within each cell, the majority of transects show a similar trend of lower RMSE value for the 13 year interval (Table 3). When RMSE values are estimated for the entire cell (e.g. for 18 transects of LC1, 16 transects for LC2 etc), it is observed that RMSE values vary from cell to cell. For some cells, viz., LC1, LC6 and LC7, the RMSE values are less for the 30 year interval; whereas for other cells, viz., LC2, LC3, LC4 and LC5, the RMSE values are less for the 13 year interval. On the other hand, when RMSE values are considered regionally, it is seen from Table 3 that RMSE values are close to each other for both 13 year interval (198.6 m) and 30 year interval (191.5 m).

The interpreted results of RMSE values can be correlated with geomorphological observations. It is seen in Table 2 that transects (viz., tr1.14, tr1.15, Tr1.S1, tr2.9, tr2.11, tr6.2, tr6.3, tr6.12, tr7.1, TR7.S1, tr7.15, tr7.16) which are closer to active natural processes (spits, marsh, inlet movements, mudflat advancement) show lower RMSE values for 30 year interval, while transects (viz., tr1.5 to tr1.13, tr2.7, tr2.8, tr2.12, tr3.1 to tr3.4, tr4.1 to tr4.4, tr6.5 to tr6.7, tr7.2 to tr7.4, tr7.12, tr7.13) which are closer to anthropogenic activities (tourism; beach transportation; land reclamation by sand mining, salt-panning and fisheries; construction of groins, seawall and flood protection embankments; inlets with lock-gates; and dumping of gabions and sandbags) show lower RMSE values for the 13 year interval (Fig. 9). As seen in Fig. 9, RMSE values are lower for thirteen year interval (1990) at transects, tr3.4 and tr4.1 for region I and at transects, tr6.5 and tr6.6 for region II, which are nearer to regions affected by anthropogenic interventions. The similar trend is also seen when RMSE values are compared littoral cell-wise. On the other hand, RMSE values are lower for the 30 year interval for transects tr6.3 and tr6.4 for region II, which are in the regions unaffected by anthropogenic activities.

Further, as seen from Tables 2 and 3, natural processes predominate in cells showing lower RMSE values for the 30 year interval (e.g.,

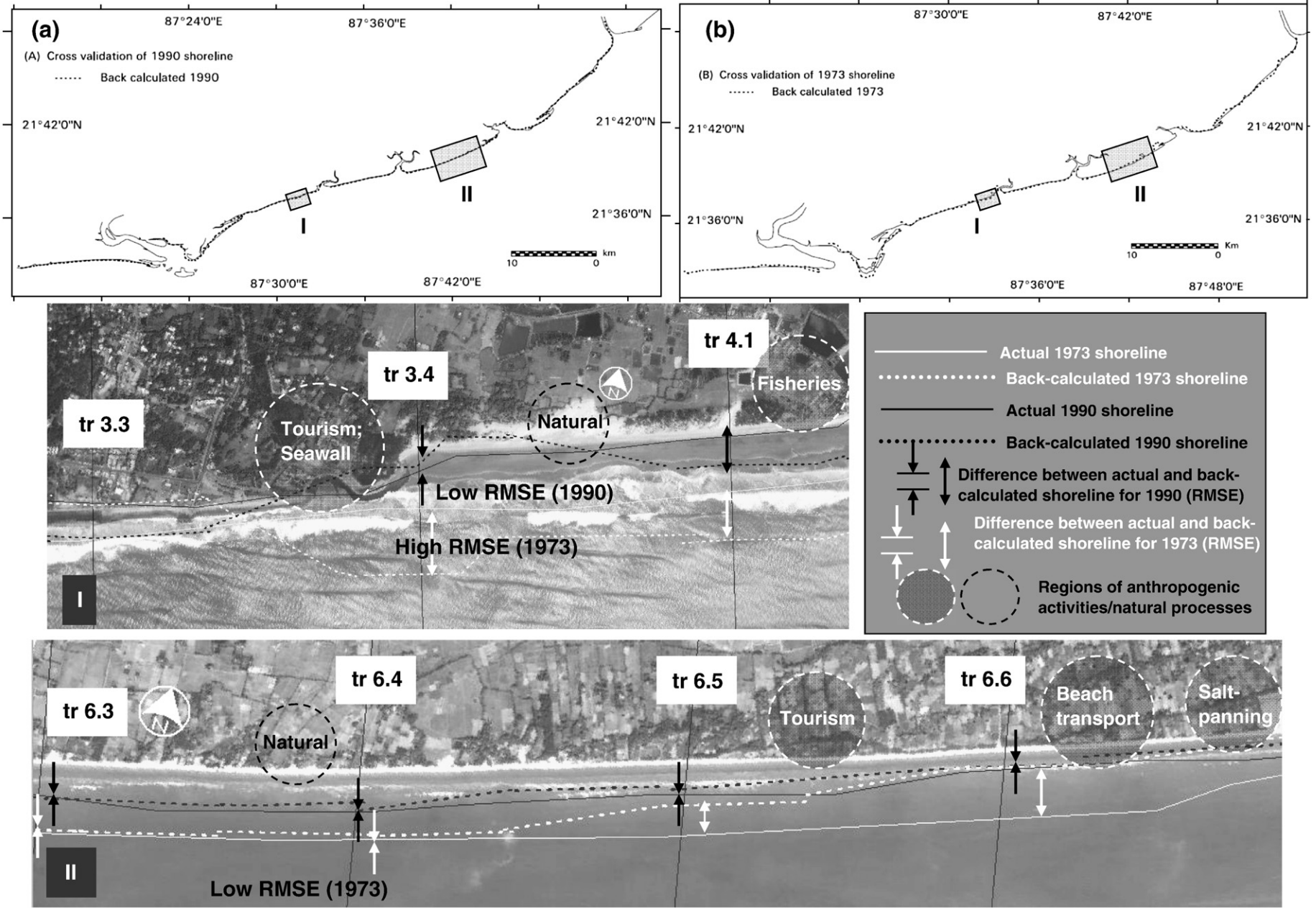


Fig. 9. Root Mean Square Error (RMSE) between back-calculated and actual shoreline positions for (a) 13 years back (1990) and (b) 30 years back (1973). RMSE estimates for the two periods (1990 and 1973) shown together for the two regions, I and II. The effects of anthropogenic activities on the RMSE estimates for different periods are highlighted.

LC1, LC6 and LC7), while anthropogenic activities are more in the other group of cells (LC2 to LC5) showing lower RMSE values for 13 year interval. This cell-wise difference of RMSEs, between the 13 and 30 years may also be related to the differences in cell lengths and hence to the number of transects within each cell; as seen in Table 3, the lower values of RMSE for the 13 year interval are for cells (LC2 to LC5) with smaller length and lesser number of transects, whereas lower values of RMSE for the 30 year interval are for longer cells (LC1, LC6 and LC7) having larger number of transects. When regionally considered, both natural and anthropogenic processes are equally effective, and therefore, RMSEs for the two periods are close to each other.

The above discussion of RMSE leads to the conclusion that short term prediction will be appropriate for the coasts subjected to anthropogenic activities, while long term prediction can be done for undisturbed coasts.

#### 4. Conclusions

The primary objective of the study was to find the applicability of multi-resolution satellite data along with statistical techniques in the prediction of shoreline changes. The present study has been carried out by finding shoreline change rates using satellite data of coarser resolution and at longer intervals by applying linear regression method. The past shoreline positions were calculated based on the derived shoreline change rates, which were cross-validated using Root Mean Square Error (RMSE). The cross-validated results indicate that shorter time intervals can be used for reliable estimates of the shoreline positions for the regions affected by anthropogenic interventions, while longer time interval can be used for reliable estimates for unaffected regions. Based on the present study, it can be concluded that accurate prediction of shoreline changes can be done cost-effectively using satellite data of higher resolution at smaller intervals and selecting short spaced transects.

#### Acknowledgements

The authors sincerely thank Global Land Cover Facility (GLCF), Land Processes Distributed Active Archive Center (LPDAAC) and Google Earth for providing free satellite data. The first author thanks Council of Scientific and Industrial Research (CSIR) India, for providing Fellowship during this study. The authors thank Ms. J. Rosati, USACE, Dr. S. Dey, Tripura University, Dr. P.K. Srivastav, IIT Kharagpur and Mr. J. B. Nanda, IIT Kharagpur for their valuable suggestions at various stages of the research work. The authors acknowledge with thanks the comments and valuable suggestions from the editor and anonymous reviewers. Partial financial support under Respond Program (ISRO, DOS, Govt. of India) is also acknowledged.

#### References

- Al Bakri, D., 1996. Natural hazards of shoreline bluff erosion: a case study of Horizon View, Lake Huron. *Geomorphology* 17, 323–337.
- Allan, J.C., Komar, P.D., Priest, G.R., 2003. Shoreline variability on the high-energy Oregon Coast and its usefulness in erosion-hazard assessments. *J. Coast. Res.* 38 (S1), 83–105.
- Bhandari, G., 2001. Coastal defence strategy and its impact on coastal environment. *Indian J. Geogr. Environ.* 6, 38–53.
- Boak, E.H., Turner, I.L., 2005. Shoreline definition and detection: a review. *J. Coast. Res.* 21 (4), 688–703.
- Bruun, P., Mehta, A.J., Johnson, I.G., 1978. Stability of tidal inlets. *Theory and Engineering*. Elsevier, Amsterdam, p. 506.
- Cooper, N.J., Hooke, J.M., Bray, N.J., 2001. Predicting coastal evolution using a sediment budget approach: a case study from southern England. *Ocean Coast. Manag.* 44, 711–728.
- CEM-II-6, 2002. Hydrodynamics of Tidal Inlets. Coastal Engineering Manual Part-II (6). U.S. Army Corps of Engineers, Vicksburg, MS.
- Coyne, M.A., Fletcher, C.H., Richmond, B.M., 1999. Mapping coastal erosion and hazard areas in Hawaii: observations and errors. *J. Coast. Res.* 28, 171–184.
- Dey, S., Dutta, S., Adak, S.B., 2002. Holocene sea level changes along the West Bengal Coast. *Indian Geogr. J.* 77 (1), 7–20.
- Dolan, R., Fenster, M.S., Holme, S.J., 1991. Temporal analysis of shoreline recession and accretion. *J. Coast. Res.* 7 (3), 723–744.
- Douglas, B.C., Crowell, M., 2000. Long-term shoreline position prediction and error propagation. *J. Coast. Res.* 16 (1), 145–152.
- Douglas, B.C., Crowell, M., Leatherman, S.P., 1998. Considerations for shoreline position prediction. *J. Coast. Res.* 14 (3), 1025–1033.
- Fenster, M.S., Dolan, R., Elder, J.F., 1993. A new method for predicting shoreline positions from historical data. *J. Coast. Res.* 9 (1), 147–171.
- FitzGerald, D.M., Kraus, N.C., Hands, E.B., 2000. Natural mechanisms of Sediment Bypassing at Tidal Inlets. CHETN-IV-30. U.S. Army Corps of Engineers, Vicksburg, MS.
- Gourlay, M.R., 1996. Wave set-up on coral reefs. 2. Set-up on reefs with various profiles. *Coast. Eng.* 28, 17–55.
- GSI, 1995. Unpublished Report on the coastal zone management plan of Digha Planning area, Medinipur District, West Bengal. GSI Operation.: WB-SIK-AN, Eastern Region Environmental Geology Divisions- II.
- Hengl, H., 2006. Finding the right pixel size. *Comp. Geosci.* 32, 1283–1298 (<http://spatial-analyst.net>).
- Israel, S.A., Carman, R.A., Helfert, M.R., Duggin, M.J., 1997. Image registration issues for change detection studies. Second Annual Conference of GeoComputation '97 & SIRCS '97, University of Otago, New Zealand, 26–29.
- Jantunen, H., Raitala, J., 1984. Locating shoreline changes in the Porttipahta (Finland) water reservoir by using multitemporal landsat data. *Photogrammetria* 39, 1–12.
- Lafon, V., Froidefonda, J.M., Lahetb, F., Castaing, P., 2002. SPOT shallow water bathymetry of a moderately turbid tidal inlet based on field measurements. *Remote Sens. Environ.* 81, 136–138.
- Lee, J.-S., Jurkevich, I., 1990. Coastline detection and tracing in SAR images. *IEEE Trans. Geosci. Remote Sens.* 28 (4), 662–668.
- Loos, E.A., Niemann, K.O., 2002. Shoreline feature extraction from remotely sensed imagery. *Geoscience and remote sensing symposium, 2002. IGARSS '02. IEEE Int. Conf.* 6 (24–28), 3417–3419.
- McBride, R.A., Taylor, M.J., Byrnes, M.R., 2007. Coastal morphodynamics and Chenier-Plain evolution in southwestern Louisiana, USA: a geomorphic model. *Geomorphology* 88 (3–4), 367–422.
- Niyogi, D., 1970. Geological background of beach erosion at Digha, West Bengal. *Bull. Geol. Min. Metall. Soc. India* 19, 191–195.
- Pajak, M.J., Leatherman, S., 2002. The high water line as shoreline indicator. *J. Coast. Res.* 18, 329–337.
- Paul, A.K., 2002. Coastal Geomorphology and Environment: Sundarban Coastal Plain, Kanthi Coastal Plain and Subarnarekha Delta Plain. acb Publication, Kolkata.
- Paul, S.K., 2006. Issues in Coastal Zone Management of Digha-Shankarpur Coastal Area. ISRO-RSAM Project Report, RRSSC, Kharagpur.
- Ryu, J.-H., Won, J.-S., Min, K.D., 2002. Waterline extraction from Landsat TM data in a tidal flat: a case study in Gosmo Bay, Korea. *Remote Sens. Environ.* 83, 442–456.
- SAC, 1992. Coastal Environment, Scientific Note, RSAM/SAC/COM/SN/11/92, Space Application Centre (ISRO), May 1992.
- Sanderson, P.J., Eliot, I., 1999. Compartmentalisation of beachface sediments along the southwestern coast of Australia. *Mar. Geol.* 162, 145–164.
- Scott, D.B., 2005. Coastal changes, rapid. In: Schwartz, M.L. (Ed.), *Encyclopedia of coastal sciences*. Springer, The Netherlands, pp. 253–255.
- Sherman, D.J., Bauer, B.O., 1993. Coastal geomorphology through the looking glass. *Geomorphology* 7, 225–249.
- Short, A.D., 2001. *Handbook of Beach and Shoreface Morphodynamics*. John Wiley and Sons Ltd, New York.
- Siddiqui, M.N., Maajid, S., 2004. Monitoring of geomorphological changes for planning reclamation work in coastal area of Karachi, Pakistan. *Adv. Space Res.* 33, 1200–1205.
- Singh, O.P., 2002. Interannual variability and predictability of sea level along the Indian coast. *Theor. Appl. Climatol.* 72, 11–28.
- Shore Protection Manual (SPM) 4 (2). U.S. Army Engineer Waterways Experiment Station. Coastal Engineering Research Centre, U.S. Government Printing Office, Washington, DC.
- White, K., El Asmar, H.M., 1999. Monitoring changing position of coastlines using Thematic Mapper imagery, an example from the Nile Delta. *Geomorphology* 29, 93–105.
- Yamano, H., Shimazaki, H., Matsunaga, T., Ishoda, A., McClennen, C., Yokoki, H., Fujita, K., Osawa, Y., Kayanne, H., 2006. Evaluation of various satellite sensors for waterline extraction in a coral reef environment: Majuro Atoll, Marshall Islands. *Geomorphology* 82, 398–411.
- Zuzek, P.J., Nairn, R.B., Thieme, S.J., 2003. Spatial and temporal consideration for calculating shoreline change rates in the Great Lakes Basin. *J. Coast. Res.* 38, 125–146.